Electronic energy structure of amorphous silicon*

W. Y. Ching, Chun C. Lin, and David L. Huber
Department of Physics, University of Wisconsin, Madison, Wisconsin 53706
(Received 11 March 1976)

By using the method of orthogonalized linear combinations of atomic orbitals (OLCAO), a first-principles calculation of the electronic energy of amorphous silicon has been performed. The lattice model used is Henderson's quasiperiodic continuous random tetrahedral network (CRTN) with 61 atoms per unit cell. The potential function is contructed from a superposition of the atomic potentials of Si at each site with a Slater-type exchange approximation. The basis functions consist of the $3s$- and $3p$-type Bloch sums for each atom in the unit cell orthogonalized to all the $1s$, $2s$, $2p$ Bloch sums so that the latter can be deleted from the basis set. All the multicenter integrals occurring in the Hamiltonian matrix elements are evaluated exactly by means of the Gaussian technique and the summation of the multicenter integrals over the lattice is carried to convergence. The calculated density of states (DOS) of the valence band is in good agreement with the experimental data. No intrinsic gap is found in this calculation but the DOS near the Fermi level is very small. Local maxima in the DOS are found to be present both above and below the Fermi level. As an alternative scheme, we have also performed OLCAO calculations based on configurational average of clusters generated from Henderson's CRTN instead of covering the entire quasicrystal as done by using Bloch-sum functions. The undesirable surface effect in cluster calculations is circumvented by taking the Hamiltonian as that of the infinite solid. The resulting DOS are compared with that obtained from the quasicrystal calculations in order to assess the accuracy of the cluster approach.

I. INTRODUCTION

In recent years the study of amorphous semiconductors has attracted considerable attention.[1-3] This is partly due to the potential technological applications of this class of materials and partly due to the new challenge to acquire a basic understanding of disorder solids. Experimental measurements of radial distribution functions (RDF) have furnished important information about the structural aspects of amorphous semiconductors.[4] Much of the recent studies seem to favor the continuous random-tetrahedral-network (CRTN) model which well accounts for the experimental RDF of amorphous Si(a-Si) and a-Ge.[2,3] Several CRTN have been built and refined.[5-11] They have different topological properties as to the number of odd-numbered rings, bond-length and bond-angle distortions, but one common feature among them is the approximate local tetrahedral coordination. The availability of structural models makes it possible to perform detailed studies of the electronic structures of a-Si and a-Ge. However, most of the previous calculations on this subject either are based on simple model Hamiltonians with various approximations or resort to empirical or semiempirical means.[2,3,12] Discussions of energy spectra of a-Si and a-Ge based on the energy-band structure of crystalline polytypes have also been given.[13-15] The results of these works have provided a great deal of insight to the problems of amorphous systems on a qualitative level. However, to delineate the finer details of electronic properties of amorphous semiconductors such as band tailing and band gap and to help interpreting experimental data, accurate first-principles calculations of the electronic energies based on realistic structural models are desirable.

The method of linear combinations of atomic orbitals (LCAO), or the method of tight binding, has been used very successfully for energy-band calculations for crystals in the past few years.[16-27] The difficulty of evaluating multicenter integrals which had been the barrier of quantitative application of this method, has been resolved by the introduction of the technique of Gaussian-type orbitals[17] (GTO). As a result the Hamiltonian matrix elements can be computed accurately and efficiently. The LCAO method has been applied to crystals of different varieties[17-27] and has been demonstrated as an effective and accurate means of calculating energy bands.

The concept of using LCAO to represent electronic wave functions in polyatomic systems is, of course, not limited to crystals and therefore should be applicable to amorphous solids. In particular, if we adopt Henderson's CRTN which consists of a quasiperiodic lattice with 61 atoms per unit cell, the problem of a-Si becomes formally identical to that of band structure of a very complex crystal. The periodicity of this model enables one to deal with a truly infinite array, thereby eliminating the surface states. The Henderson model[8] has larger bond-angle and bond-length distortion than some of the other CRTN models;

nevertheless it reproduces quite well the experimental RDF and is found to be quite successful in lattice-vibration calculations. Although theoretically the basic principles behind an LCAO calculation for a crystal of 61 atoms per unit cell are no different from those for simpler crystals, in practice the computational procedure must be carefully economized so that the numerical work does not become unduly excessive. A brief report of our efforts on a first-principles LCAO calculation of the electronic structure of a-Si based on Henderson's CRTN model has been published.[28] The potential for the one-electron Hamiltonian is obtained by the usual overlapping-atomic-potential (OAP) approximation, i.e., a superposition of the individual free-atom potentials (with a Slater-type approximation for exchange) at the appropriate sites. With the Bloch sums of the atomic orbitals as basis functions, all the Hamiltonian matrix elements can be readily computed by means of the Gaussian technique. The limiting factor, however, was the size of the secular equations as even a minimal set of $1s, 2s, 2p, 3s, 3p$ orbitals for each atom would lead to 549 basis functions. Thus in Ref. 28 the $1s, 2s, 2p$ core-state Bloch sums were deleted from the basis set. The omission of core states in an LCAO expansion of the electronic wave functions may at times cause a serious collapse of the energy levels because the eigenvalues of the secular equations would tend to converge toward the core states instead of the valence states. For the specific case of Ref. 28, this approximation has little effect on the states near the top of the valence band, but does produce a much larger downward shift for the lower-energy levels in the valence band. The results of Ref. 28 compare favorably with the experimental data and also reveal some interesting features of the density of states (DOS) near the Fermi level.

In this paper we improve our previous calculations by orthogonalizing the $3s$ and $3p$ Bloch sums to all the core Bloch sums and using these $3s$ and $3p$ orthogonalized Bloch sums in place of the unorthogonalized ones as the basis functions to set up the 244×244 secular equations. The scheme of orthogonalized linear combinations of atomic orbitals (OLCAO) has been recently applied to study the band structure of Si III.[29] In that work the band energies of Si III were calculated by using the OLCAO method and by using the usual LCAO method with all the core states included. The two sets of energies differ by no more than 0.0008 a.u., confirming the accuracy of the OLCAO method. For the a-Si problem, the OLCAO calculation does lift the energies of the valence-band levels, especially the lower ones, upward as compared to Ref. 28 (see Sec III), resulting in a better agreement with experiment. Details of this calculation are described in Sec. II and the results are discussed in Sec III.

As the validity of the LCAO method does not depend on the periodicity of the structural model, it is interesting to explore also its application to the cases in which no quasiperiodicity is assumed. In the absence of periodicity, we can no longer include the entire infinite array of atoms in our basis functions, and a practical alternative is to treat only finite clusters out of the infinite solid. One can voice a reservation about the cluster approach because the artificial surface of the cluster introduces a number of surface states which are not present in the infinite (nearly) CRTN. The difficulty with the surface states has been resolved in a recent study of cluster calculations for the perfect silicon crystal.[30] It is pointed out there that the surface states would not appear if in the cluster calculation the basis functions are limited to localized orbitals centered at atomic sites within a cluster, but the potential term in the one-electron Hamiltonian includes the contribution of all the atoms in the infinite solid so that no real physical surface is present in the Hamiltonian. Indeed the energy spectrum of the perfect Si crystal obtained by such a cluster calculation agrees well with the results of the LCAO Bloch-sum calculation. We shall, therefore, apply this technique of cluster calculation to a-Si. Specifically from Henderson's CRTN we select a cluster of atoms and calculate the energy levels using the atomic orbitals associated with this cluster as the basis, and the calculation is then repeated for a number of clusters from the same CRTN. The average DOS of these clusters is compared with the one determined from the quasicrystal calculation to assess the accuracy of the cluster approach. Section IV of this paper is devoted to this aspect of the work.

II. METHOD OF CALCULATIONS

With the Henderson CRTN model, the problem of amorphous silicon is reduced to that of the band structure of a crystal (simple cubic) with 61 atoms in a unit cell. To start an LCAO calculation one must have available a set of basis functions and a potential. For the present work, they are chosen in a manner similar to that described in our earlier papers[28,29]; thus only a brief account is given here.

In the conventional LCAO method, the basis functions consist of the Bloch sums of the atomic orbitals corresponding to the core and valence shells. To simplify the numerical computation, these orbitals are expanded by GTO's.[17] Such a

basis set is quite adequate for the valence band and the lower conduction band. However, it is not necessary to confine oneself to the true wave functions of the free atom. In fact more accurate energy-band results can be obtained if the true orbitals of the free atoms were replaced by some localized functions ϕ_i which are qualitatively similar to the true atomic wave functions but include to some extent the distortion of the electron cloud by the other atoms in the crystal. Such a set of optimized orbitals can be obtained by the technique of contracted Gaussian described by Simmons *et al.*[31] Based on their procedure we have constructed a set of $1s$, $2s$, $2p$, $3s$, $3p$ optimized orbitals for Si which are given in Ref. 29 and are used here. Returning to the quasicrystal, let us denote the position of the αth atom in the unit cell by $\vec{\rho}_\alpha$ and a translation vector of the lattice by $\vec{R}_\nu$. Associated with each atom in the unit cell one can form nine Bloch sums as

$$b_{i\alpha}(\vec{k},\vec{r}) = \sum_\nu e^{i\vec{k}\cdot R_\nu}\,\phi_i(\vec{r}-\vec{\rho}_\alpha-\vec{R}_\nu)\ , \tag{1}$$

where $i = 1s, 2s, 2p, 3s, 3p$ and α ranges from 1 to 61. This set of 549 basis functions is too large to handle; hence we seek to orthogonalize the $3s$ and $3p$ Bloch sums to the core states so that the latter can be excluded. Following the procedure of Ref. 29, we introduce the orthogonalized Bloch sums as

$$b'_{q\alpha}(\vec{k},\vec{r}) = b_{q\alpha}(\vec{k},\vec{r}) + \sum_{\gamma=1}^{61}\sum_{l=1s}^{2p} a_{q\alpha,l\gamma}\, b_{l\gamma}(\vec{k},\vec{r})\ , \tag{2}$$

where q is restricted to $3s$ and $3p$ only. The coefficients $a_{q\alpha,l\gamma}$ are determined by the orthogonality conditions. With only the valence orbitals for each atom, we have 244 orthogonalized Bloch sums which are used as the basis functions for our calculations.

The potential in the one-electron Hamiltonian can be expressed as a superposition of some atomic-like potential V_a centered at each Si site. In our calculation V_a is approximated by the potential (spherical) of a free Si atom computed from the atomic Hartree-Fock wave function (using a Slater-type local exchange with $\alpha = \frac{2}{3}$)—sometimes referred to as the overlapping-atomic-potential (OAP) approximation. To test this potential we employ the same V_a along with the OAP approximation to calculate the band structure of crystalline Si and the results are in good agreement with those of Stukel and Euwema.[32] For the ease of computation, the atomic potential (including both the Coulomb and exchange parts) is fitted to the following form:

$$V_a(r) = -\frac{Z}{r}\,e^{-Cr^2} + \sum_i \xi_i\, e^{-b_i r^2}\ . \tag{3}$$

The first term in the above equation simulates the small-r behavior of the Coulomb potential. Usually eight or nine Gaussians are sufficient to provide a good fit up to a radial distance of 6–7 a.u. With the Bloch sums as basis functions, a typical potential-energy matrix element can be decomposed into a series of three-center integrals containing a Gaussian centered at point A, another one at B, and the atomic potential V_a around C. The integrals associated with the first term of Eq. (3) can be expressed in terms of the error function and those associated with the second member can be evaluated analytically. An outline of the computational procedures involved is presented in the Appendix. For energy-band calculations the very long-range component of the atomic potential can be suppressed with virtually no change in the band structure. This procedure has the advantage of a substantial reduction of the computation work and is adopted here. The parameters of the Gaussian fit are given in Ref. 29.

A typical Hamiltonian matrix element is expanded as a lattice-point summation of multicenter integrals. This lattice summation must be carried out to full convergence. To illustrate the rate of convergence, we cite a typical case as follows: $\langle\phi_{3s}(\vec{r}-\vec{A})\,|H|\,\phi_{3s}(\vec{r}-\vec{B})\rangle = -0.5939$, -0.1809, -0.0224, -0.0045, -0.0004 a.u., respectively, for $|\vec{A}-\vec{B}| = 0$, 4.443 (first nearest neighbor), 7.255 (second nearest neighbor), 8.508 (third nearest neighbor), 10.258 a.u. (fourth nearest neighbor). For an amorphous solid, the neighbor distances are not constant; thus the above numbers merely give a rough indication of the magnitude of the integrals between various neighbor pairs. Upon computing all the Hamiltonian (H_{ij}) and overlap (S_{ij}) matrix elements, the energy spectrum is obtained by solving the secular equations $|H_{ij} - ES_{ij}| = 0$ for various $\vec{k}$ points. Because of the truncation errors involved in solving secular equations of dimension as large as 244, the matrix elements must be computed to a much higher degree of precision than the desired accuracy of the eigenvalues. In the present work the lattice summation is carried out to typically the eighth neighbors. The Hamiltonian matrix elements themselves typically reach their ultimate values to within about 0.1% when the contributions of the atoms within a distance less than or equal to the fourth neighbors of the corresponding crystal are included. One can probably get satisfactory results for the coarse features of the energy spectrum of the occupied states

by retaining up the fourth-neighbor terms in the lattice summation, although we have not made any quantitative test.

III. RESULTS AND COMPARISON WITH EXPERIMENTS

We obtain the energy levels by solving the 244 $\times$244 secular equations for four high-symmetry $\vec{k}$ points [$\pi(0,0,0)/a$, $\pi(1,0,0)/a$, $\pi(1,1,0)/a$, $\pi(1,1,1)/a$] and seven other $\vec{k}$ points: $\pi(\frac{1}{2},0,0)/a$, $\pi(\frac{1}{2},\frac{1}{2},0)/a$, $\pi(\frac{1}{2},\frac{1}{2},\frac{1}{2})/a$, $\pi(1,\frac{1}{2},0)/a$, $\pi(1,\frac{1}{2},\frac{1}{2})/a$, $\pi(1,1,\frac{1}{2})/a$, and $\pi(\frac{3}{4},\frac{2}{4},\frac{1}{4})/a$. The energy matrices are real for the first group of $\vec{k}$ points but are complex for the second group. The top of the valence band is found to be at $\vec{k}=0$ and the bottom of the conduction band at $\vec{k}=\pi(1,1,1)/a$. The latter is lower than the former by 0.11 eV and this is the only point (out of the 11 $\vec{k}$ points calculated) where the conduction band falls below the top of the valence band. However, one should bear in mind that this band gap is obtained by using a minimal basis-function set. An augmentation of the basis set, such as addition of single-Gaussian Bloch sums, may shift the conduction-band and valence-band edges differently. Improvement of the crystal potential to self-consistency could also change the band gap. Furthermore, the uncertainty in the CRTN model may well exceed the accuracy of a fraction of an eV. Taking all these into consideration, we conclude that for a void-free and impurity-free a-Si, the band gap, if it exists, is very small and a negative intrinsic gap is a distinct possibility.

Instead of focusing our attention to the band gap, it is more informative to examine the DOS. Since the Brillouin zone (BZ) for the 61-atom quasiperiodic lattice has no point-group symmetry, in principle one has to calculate the energy levels for $\vec{k}$ points over the entire zone. However, in view of the small deviation from the perfect diamond lattice and of the large number of atoms in the unit cell, we assume an effective cubic symmetry for the BZ, insofar as the overall energy-level distribution is concerned, so that we can confine our calculation to a fundamental wedge of the BZ in order to reduce the computation work. This assumption is supported by test calculations which show that the DOS associated with the $\pi(1,0,0)/a$ and $\pi(1,1,0)$ points is indeed quite similar to that associated with $\pi(1,0,0)/a$, $\pi(0,1,0)/a$, $\pi(0,0,1)/a$, $\pi(1,1,0)/a$, $\pi(1,0,1)/a$, and $\pi(0,1,1,)/a$. Accordingly we take the calculated energy levels of the eleven $\vec{k}$ points mentioned above and use an interpolation procedure to obtain energy levels for 35 regularly spaced k points in the fundamental wedge of the BZ. Here we expand the energy of a $\vec{k}$ point as

$$E(\vec{k}) = E_0 + E_2k^2 + k^4(E_4 + E_4'K_{4,1}) + k^6(E_6 + E_6'K_{4,1} + E_6''K_{6,1}),$$

where K_{41} and K_{61} are, respectively, the fourth- and sixth-Kubic harmonics[33] which transform according to the identity representation. The coefficients E_0, E_2, etc. are determined by a least-square fit to the calculated energies of the eleven $\vec{k}$ points. The rms deviation of this fit is about 0.0007 a.u. With the energy values deduced for the 35 $\vec{k}$ points, a simple histogram counting procedure is used to obtain the DOS which is shown in Fig. 1. The general shape is similar to the one reported in Ref. 28 except that the energies of the lower part of the valence band shown in Fig. 1(b) of Ref. 28 are shifted upward as a result of the proper treatment of the core states. This improves the agreement of the calculated DOS of the valence band with the measurement of Ley *et al.*[34] which is represented in Fig. 1 by a smooth curve normalized to match the height of the leading peak of the theoretical DOS. The huge peak in the upper portion of the valence band is retained, while the lower one is on the verge of evolving into two subpeaks. Small structures are seen all over the valence band as well as the conduction band. The positions of these small structures would undoubtedly vary from model to model. If one were to represent a-Si as a certain distribution of different models, these small structures may be broadened or in some cases merge. Aside from the small structures, the envelope of the conduction-band DOS shows only one clear-cut peak. This is consistent with the observation of Brown and Rustgi.[35] The calculated energies of the levels at the upper

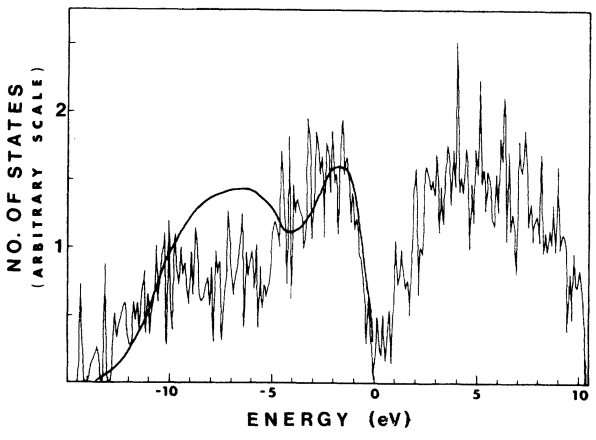

FIG. 1. Comparison of the calculated DOS of the conduction and valence bands of a-Si (the rapidly varying curve) with the experimental valence-band DOS (the smooth curve) of Ref. 34. The experimental curve is normalized to match the leading peak of the theoretical curve.

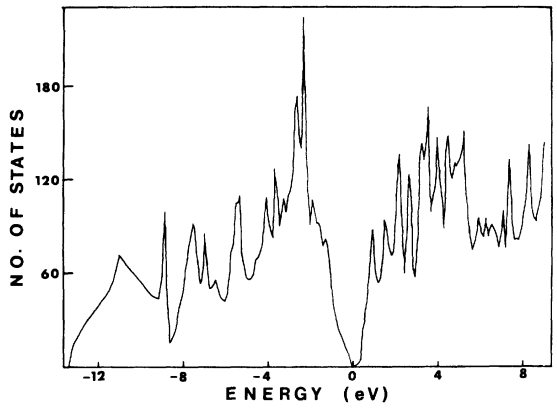

FIG. 2. Theoretical DOS of the conduction and valence bands of Si III calculated by the OLCAO method (Ref. 29).

part of the conduction band are less accurate than the lower states because the basis set contains only the minimal 3*s* and 3*p* orbitals with no single-Gaussian supplements.

As a reference point for comparison let us turn our attention to the DOS of Si III given in Ref. 29, which is reproduced in Fig. 2 here. While there is little resemblance with *a*-Si as far as the general shape is concerned, one does find many small structures in the DOS of Si III (eight atoms per unit cell), though not as numerous as in *a*-Si. This leads us to believe that the small structures are related to the distortion from perfect tetrahedral coordination in the lattice. One point of special interest is the presence of small peaks in the DOS immediately below and above the Fermi surface for *a*-Si but not for Si III even under very detailed examination. This feature clearly distinguishes the *a*-Si from the polytype crystalline forms. Experimental evidence for the presence of local maxima in the DOS near the Fermi level has been found from optical and electrical measurements;[36-38] these maxima are usually interpreted as being connected with localized states. In principle, we can determine whether or not the small peaks near the Fermi level in Fig. 1 are due to localized states by inspecting the corresponding wave functions. However, for secular equations of dimensionality as large as 244, we are able to obtain only the eigenvalues but not the eigenvectors with the local computing facilities.

To compare our results with the experimental optical band gap, it is necessary to recast the former in the context of the latter. The negative gap obtained in our calculation is not in contradiction with the observation of an optical band gap inasmuch as the DOS is very small near the Fermi level. In Fig. 3(a) is shown our calculated joint density of states (JDOS) up to 14 eV. The part of the JDOS between 0 and 2.5 eV is magnified and given in Fig. 3(b). Although in principle the $\vec{k}$ selection rule holds for a true 61-atom periodic lattice, we do not apply it to our calculation of JDOS as any deviation from exact quasiperiodicity in reality would remove this restriction. Below 0.6

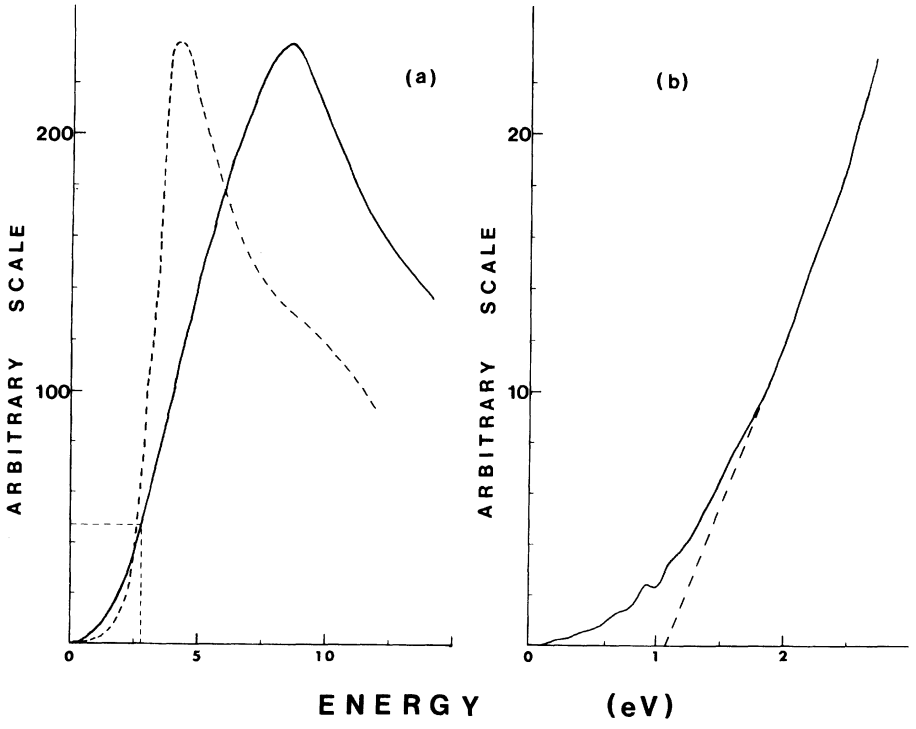

FIG. 3. (a) Comparison of the calculated JDOS of *a*-Si from 0–14 eV (solid curve) with the experimental optical-transition strength from Ref. 40 (dotted curve). The two curves are adjusted to have the same maximum height. (b) The portion of the calculated JDOS enclosed inside the rectangle in (a) is magnified in part (b) to illustrate the small peak at 0.9 eV. Extrapolation of the linear part of the curve about 1.7 eV to lower energies is shown by the dotted line.

eV the JDOS becomes very small. If one were to perform measurements between, say, 1.7 and 2.5 eV and extrapolate to lower energies, one would arrive at a band gap of about 1.1 eV. The small peak at 0.9 eV in Fig. 3(b) originates from the local maxima in the DOS (Fig. 1). It may be pointed out that a peak at 1.1 eV in the experimental data of absorptance[39] has been reported. Quantitative comparison, however, will not be attempted because of the absence of a detailed knowledge of the transition matrix elements. Likewise, included in Fig. 3(a) is the experimental optical-transition curve[40] normalized to the same maximum height as the theoretical JDOS for the purpose of illustrating the similar *qualitative* trend.

IV. CLUSTER-TYPE CALCULATIONS

If the CRTN model is not quasiperiodic, the formalism described in Sec. II in which the basis functions are the Bloch sums corresponding to the quasiperiodic structure, is no longer applicable. For a nonperiodic CRTN, one may resort to a cluster approach. A number of theoretical calculations for amorphous semiconductors based on cluster models have been published.[12] In particular the LCAO scheme has been used in conjunction with a cluster calculation in which the matrix elements are determined by empirical means.[41]

In approximating an infinite solid by a finite polyatomic cluster, the presence of the surface of the cluster produces some surface states which have no counterparts in the infinite solid. In principle, the number of surface atoms relative to bulk atoms decreases with increasing cluster size, yet even a 600-atom cluster generated from the Henderson model has 127 atoms with one dangling bond, 72 atoms with two dangling bonds, and 10 atoms with three dangling bonds. Only 65% of the atoms are "interior" ones. The difficulty with the surface states has been circumvented in a recent study by Menzel *et al.*[30] In their version of cluster calculation for crystalline Si, these authors used the potential of the entire infinite crystal, but their basis functions consist of localized orbitals confined within a finite cluster. In other words, they solve the one-electron Hamiltonian of an infinite crystal by means of a special truncated LCAO basis set. There is no physical surface present in the Hamiltonian; indeed their results show no surface states. However, as explained in Ref. 30, a precaution must be observed in using a finite cluster-type basis set in conjunction with a Hamiltonian of the infinite crystal. This is due to the fact that the Hamiltonian used in that work is capable of yielding an infinite number of core-state eigenvalues, but with a cluster-type basis set, one expects the eigenvalues to include the core states of only the atoms inside the cluster. If the $3s$ and $3p$ basis functions inside the cluster penetrate appreciably into the sites outside, the minimum-seeking nature of the linear variational scheme would attempt to reproduce the core states of the exterior atoms giving rise to some spurious roots. To ensure against this complication, Menzel *et al.*[30] supplement their basis functions inside the cluster with the $1s, 2s, 2p$ core orbitals around the sites in the next few exterior shells. With such a core-state cushion, they find no spurious roots and are able to reproduce quite well the density of states of the infinite crystal by a cluster-type treatment.

In this paper we follow the technique of Menzel *et al.*[30] to perform cluster-type calculations using Henderson's model. The Hamiltonian is that of the infinite CRTN. The individual atomic orbitals within a cluster are chosen as the basis functions. Instead of adding cushion core orbitals of the sites immediately outside the cluster as is done in Ref. 30, we orthogonalize the basis orbitals to the exterior core states. The latter serves the same purpose as the core cushion but does not entail an augmentation of the basis set. We also orthogonalize the basis functions to the $1s, 2s, 2p$ core states of the atoms *inside* the cluster so that these core functions can be deleted. The basis set then consists of exclusively such orthogonalized $3s, 3p$ orbitals of all the atoms inside the cluster. With the potential functions expressed as a superposition of Eq. (3), a matrix element is composed of the same kind of multicenter integrals as described in Sec. II and may be evaluated by the procedure outlined in the Appendix. In an amorphous solid, clusters taken from different parts of the CRTN are not equivalent, thus for a given cluster size we perform DOS calculations for several clusters and take the average.

The computational procedure may be summarized as follows: In the CRTN we take a volume containing some 200 atoms which is schematically represented in Fig. 4 as region A and orthogonize the $3s$ and $3p$ optimized orbitals at each site therein to all the $1s, 2s, 2p$ core states within that region. Inside region A a number of clusters (shown in Fig. 4 as C_1, C_2, etc.) are selected, and for each one we perform a cluster-type calculation of the energy levels. To ensure cushion protection, no part of the boundary of a cluster should come too close to the edge of region A. The potential-energy term in the one-electron Hamiltonian covers contribution from all atoms in the infinite CRTN. In our calculation we find that inclusion of the individual atomic potentials of all atoms in-

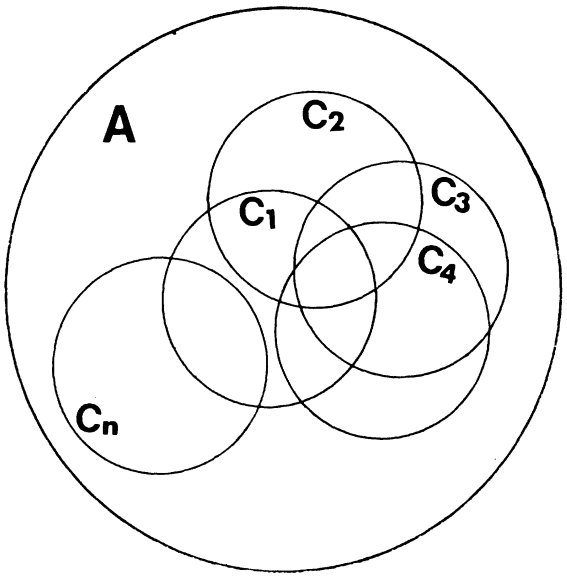

Fig. 4. Schematic diagram for region A and the various clusters C_1, C_2, etc.

side region A and of some 400 atoms outside is sufficient to represent the infinite CRTN as far as the Hamiltonian matrix elements are concerned. It is, of course, not necessary to limit region A to 200 atoms. A larger volume for region A would be even better, although it would involve more computational work.

We start with a cluster size of 17 atoms. With a given atom as the center, we include in the cluster the 16 atoms which are closest to it. In the limiting case of a perfect crystal, this corresponds to a central atom plus its first- and second-nearest neighbors. By placing the center at different atoms, we form a total of 38 clusters of the same size inside region A. The energy levels of all these 38 cluster configurations are calculated and the average DOS is shown in Fig. 5(a). The valence-band DOS does show a leading peak followed by a weaker secondary peak, but a much larger disparity in the two peaks is seen here as compared to the curve in Fig. 1 which is also reproduced in Fig. 5(d) for visual juxtaposition. The

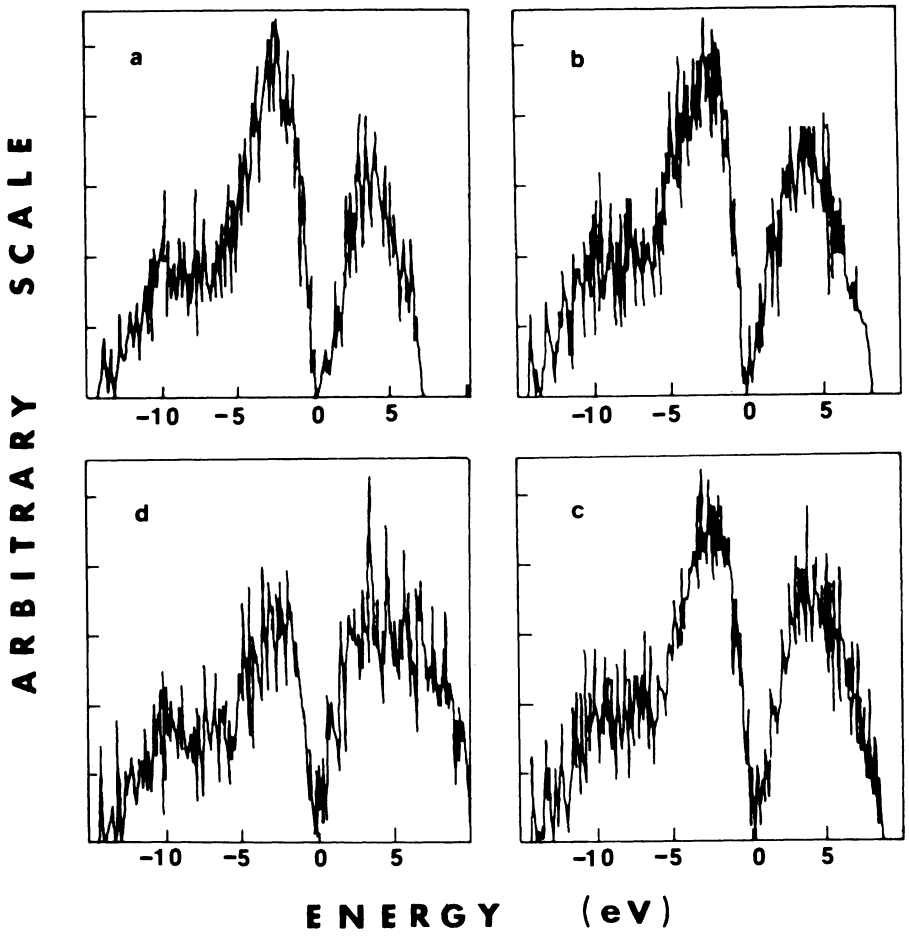

FIG. 5. Density of states of the conduction and valence bands of a-Si calculated by using the average of (a) 38 17-atom clusters, (b) 18 35-atom cluster, and (c) 10 60-atom clusters. The DOS calculated by treating the entire quasicrystal (Fig 1) is reproduced in (d) for comparison.

conduction part of Fig. 5(a), however, shows much less similarity to Fig. 5(d). This is because a cluster covering up to only the second-nearest neighbors is not capable of giving a satisfactory over-all representation of the conduction-band levels, especially the higher ones. A detailed study of this point for crystalline Si has been discussed in Ref. 30. Furthermore, in a cluster calculation one always obtains more valence-band states than conduction-band states because of the dangling orbitals of the boundary atoms.[30,42] This is indeed reflected in Fig. 5(a) as the area under the conduction branch of the DOS curve is distinctly smaller than the area associated with the valence states. For a given 17-atom cluster, we find a finite energy difference of typically 1.6 eV between the uppermost occupied level and the lowest empty one. Upon taking an ensemble of 38 clusters, the gap between the occupied and unoccupied states is reduced to 0.27 eV. We also performed similar calculations for 18 clusters with 35 atoms in each cluster and for 10 clusters with 60 atoms in each. The resulting DOS are included in Fig. 5. The improvement in going from 17-atom to 60-atom clusters is apparent. However, even the 60-atom-cluster calculation still tends to accentuate the leading peak relative to the second one in the valence band. Also the upper part of the conduction band is not well represented. One point worth remarking is the presence of the small local peaks near the Fermi level in the cluster results for all three cluster sizes.

To illustrate how the energy levels evolve with increasing cluster size, we start with a central atom and build around it a series of clusters containing 1, 5, 17, 29, 35, 47 atoms. In the limiting case of a perfect crystal, these clusters would correspond to inclusion of the central atoms only, the first-nearest neighbors, the second-nearest neighbors, and so on. The valence-type levels and the lower part of the conduction-type levels resulting from this series of cluster calculations are shown in Fig. 6. We wish to emphasize once again that the Hamiltonian is that of the infinite CRTN in all these cluster calculations. Of special interest is the case of the one-atom cluster which, in the case of a perfect crystal, would give an s-type level and a triply degenerate p-type level. The splitting of the upper three levels for the one-atom cluster in Fig. 7 reflects the departure of the potential in the proximity of the central atom from perfect tetrahedral coordination. For this specific case the distances to the four neighbor atoms relative to the nearest-neighbor separation in the perfect crystal are 0.934, 1.019, 1.037, and 1.036 and the six angles between these four bonds are 95.3°, 131.3°, 132.0°, 129.0°, 79.8°, and 88.5°, differing substantially from the perfect

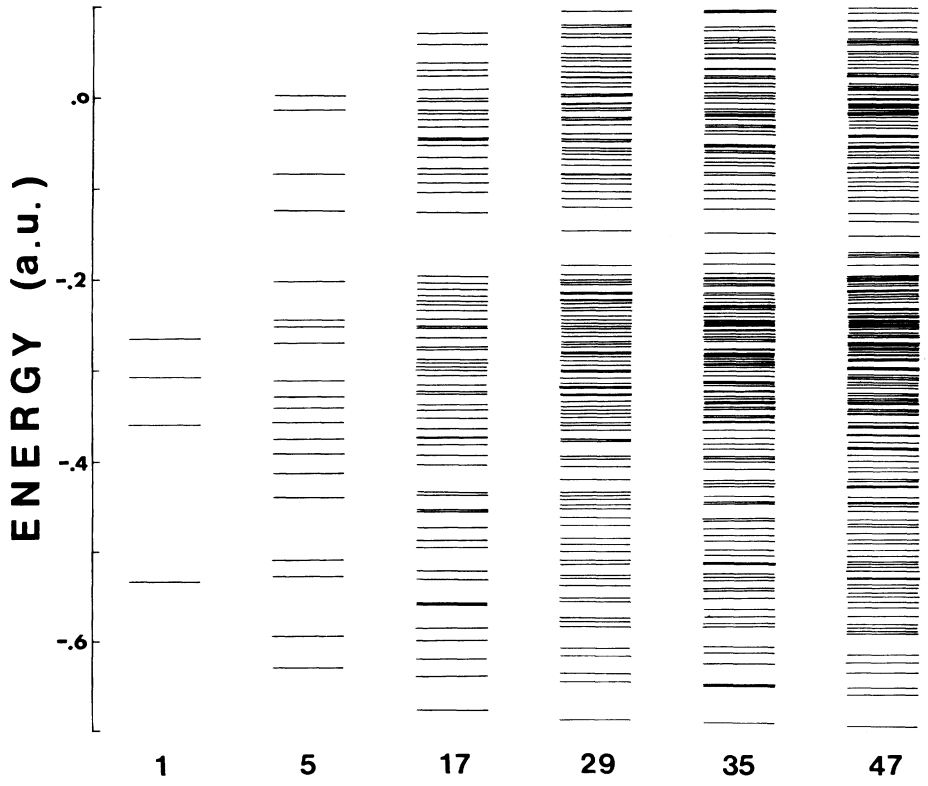

FIG. 6. Energy levels of the valence-band states and the lower conduction-band states of a-Si for clusters containing 1, 5, 17, 29, 35, 47 atoms. The zero of the energy scale is arbitrary.

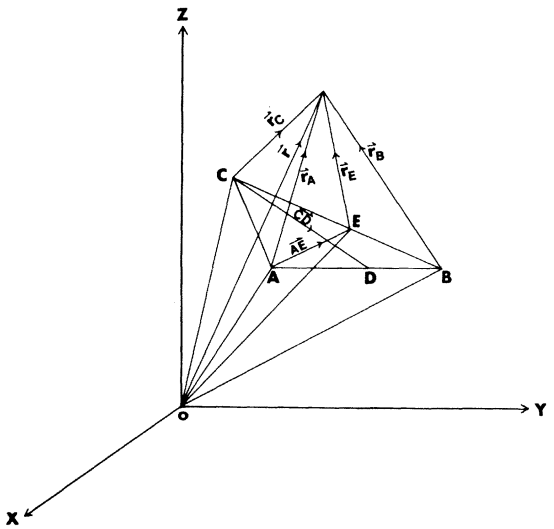

FIG. 7. Relations between the various points and vectors relevant for the reduction of multicenter integrals.

tetrahedral angle. (This point has larger local distortion than most of the others in the CRTN.) For each of the six clusters in Fig. 6, one finds a region near the top of the valence band corresponding to the leading peak in the DOS. Also clear in Fig. 6 is the gradual rise of the top of the valence group and descent of the lower boundary of the conduction group as the cluster size increases. With a 47-atom cluster, the gap between these two groups of levels is not significantly larger than some of the gaps within the valence band.

V. DISCUSSION

The electronic energy level spectrum of a-Si has been calculated by means of the method of LCAO. The Henderson quasiperiodic CRTN model with 61 atoms per unit cell is used to describe the structure of a-Si. The potential function is approximated by the OAP model. As the basis functions we form Bloch sums of $3s$ and $3p$ orbitals (optimized) associated with each of the 61 atoms in the unit cell and orthogonalize them to all 61 sets of $1s$, $2s$, and $2p$ Bloch sums. This makes a total of 244 functions constituting what is normally regarded as a minimal set. For perfect crystals such a minimal basis set generally gives quite satisfactory results. To give some perspectives of our calculations in the framework of band-structure theory, we may point out some possible refinements which can be incorporated into the present scheme. For a given one-electron Hamiltonian one can add Bloch sums of single Gaussians or contracted Gaussians to the basis set to strengthen the variational freedom thereby improving the accuracy of the eigenvalues.[31] Another direction of improvement is to proceed to a self-consistent-field calculation. Furthermore one may get a more realistic representation of a-Si by taking a superposition of a number of quasiperiodic CRTN's instead of just one. Particularly it should be interesting to study a quasiperiodic CRTN with smaller bond-length and bond-angle distortions than the Henderson model.

Our calculated valence-band DOS is in good agreement with the experimental data of Ley *et al.*[34] The general feature of two peaks in the valence band is in agreement with the previous suggestion that the leading peak found in crystalline Si should persist whereas the middle sharp peak and the bottom peak associated with the crystal valence band tend to merge into a broader peak.[43] However, the local maxima in the DOS immediately below and above the Fermi level found in our calculations have not been previously predicted from purely theoretical considerations. On the other hand, existence of such local maxima has been inferred from experiments, and they are traditionally attributed to voids or dangling bonds in the sample. The present calculations show that such structures in the DOS may be present even for a void-free, pure sample if there exist appreciably distortions of bond length and bond angles from the perfect tetrahedral configuration.

Our results show no absolute band gap for a-Si but the overlap of the two bands is very small and the DOS in this overlap region is extremely low. The precise question of whether an absolute band gap exists or not for the Henderson model cannot be settled here since the refinements of augmenting the basis set and iterating to self-consistency may well shift the edges of the bands differently resulting in a quite different gap value. Nevertheless, our results are not in conflict with those of the optical experiments as the optical gap may be considerably larger than the absolute band gap (if exists) when the DOS is very low near the Fermi level. The JDOS calculated from the DOS curve is in qualitative agreement with optical experiments, although the peak of the calculated JDOS seems to shift to the higher-energy side as compared to the experimental data of optical absorption strength. This discrepancy may be due to the energy dependence of the optical matrix elements.

We have also calculated the DOS by using a cluster approach. By taking the Hamiltonian as that of the infinite CRTN, we circumvented the difficulty associated with the presence of an artificial surface. The basis functions are confined to orbitals of those atoms within a cluster. Since different clusters of the same size are not equiv-

alent in an amorphous solid, we take the average DOS of a number of clusters. Our LCAO cluster study differs from the earlier work of Tong[41] in that our matrix elements are calculated by using first principles instead of empirical methods and that our Hamiltonian corresponds to an infinite CRTN with no surface present. By comparing the calculated DOS using clusters of three different sizes (17, 35, and 60 atoms) with the results based on the Bloch-sum basis functions, we find that the general shape for the valence band is adequately reproduced by the cluster works. The quantitative features do improve as the cluster size is increased; the 60-atom clusters give a moderately good representation of the valence-band DOS.

For a first-principles calculation of a system as complex as a-Si, it is useful to include a few comments concerning the computer time required. In the case of the quasicrystal approach (Sec. II), it takes about 60 min on a Univac 1110 machine to compute all the necessary matrix elements. Determination of the roots of a 244×244 secular equation (including the orthogonalization process) generally requires 7 min if the matrix is real and 25 min for a complex matrix. Thus for the calculation of DOS in which we solved four real secular equations and seven complex ones, the major computer-time expenditure is on the diagonalization of matrices rather than the computation of matrix elements. This indicates that the technique for evaluating multicenter integrals has advanced to the point that the computation of matrix elements is no longer a very time-consuming task. If we were to use some empirical methods to obtain the matrix elements, we would still have to diagonalize the matrices and no major saving in computer time is accomplished. Moreover, because in an amorphous solid the "nearest-neighbor" distance varies over a wide range with different degrees of bond-angle distortion, a realistic parametrization of the matrix elements is more complicated as compared to the case of a perfect crystal, making it difficult to obtain reliable results from empirical LCAO calculations for a-Si. Considering the amount of computation involved as well as the question of accuracy, we feel that the use of a first-principles approach for quantitative calculations of electronic energies of a-Si is both practical and essential.

In conclusion we have demonstrated that based on the quasiperiodic CRTN model of Henderson, a first-principles calculation of the electronic energy states of a-Si can be performed quite efficiently by means of the orthogonalized LCAO method. The quasiperiodic model is particularly suitable as it enables us to adopt the techniques developed for band-structure calculations for crystals to amorphous systems. All the multicenter integrals are computed exactly and the lattice-summation of these integrals (to form matrix elements) is carried out to convergence. Although the OAP approximation used in constructing the potential in this work can be improved upon by iterating the solution to self-consistency, this step would involve a great deal more computational efforts and is not deemed worthwhile at this moment considering the uncertainty of the CRTN model involved. It would be desirable to have other quasiperiodic models available for a comprehensive comparison. For nonperiodic CRTN one can still apply the LCAO method by adopting the cluster approach. However, care must be taken to ensure that the clusters are large enough to reproduce the salient features of the whole network. Besides pure amorphous systems, this LCAO scheme can be readily extended to study the problems of impurity and void effects in amorphous solids.

ACKNOWLEDGMENTS

The authors wish to thank K. Mednick and W. P. Menzel for their assistance throughout the course of this work and Dr. R. Alben and Dr. D. Weaire for helpful suggestions.

APPENDIX

Since the atomic wave functions are expanded by GTO's and the potential function is taken as a superposition of atomiclike potentials which in turn are expressed in Gaussian form, a potential-energy matrix element between two s-type Bloch sums can be decomposed into two kinds of three-center integrals around three sites A, B, and C, i.e.,

$$(s_A|e^{-\alpha_3 r_C^2}|s_B)\equiv(e^{-\alpha_1 r_A^2}|e^{-\alpha_3 r_C^2}|e^{-\alpha_2 r_B^2}), \tag{A1}$$

$$[s_A|(1/r_C)e^{-\alpha_3 r_C^2}|s_B] \equiv[e^{-\alpha_1 r_A^2}|(1/r_C)e^{-\alpha_3 r_C^2}|e^{-\alpha_2 r_B^2}], \tag{A2}$$

where r_A is the distance between the electron and site A, etc. We define

$$\alpha_T=\alpha_1+\alpha_2+\alpha_3, \tag{A3}$$

$$\vec{E}=(\alpha_1\vec{A}+\alpha_2\vec{B}+\alpha_3\vec{C})/\alpha_T, \tag{A4}$$

$$\overline{AE}=|\overline{A}\vec{E}|=|\vec{E}-\vec{A}|, \quad \text{etc.}, \tag{A5}$$

where $\vec{A}$ is the vector from the origin to site A. The relation between the various points and vectors is illustrated in Fig. 7. It follows that

$$\vec{r}_A=\vec{r}_E+\overline{A}\vec{E}, \quad \text{etc.}, \tag{A6}$$

$$\alpha_1\overline{A}\vec{E}+\alpha_2\overline{B}\vec{E}+\alpha_3\overline{C}\vec{E}=0, \tag{A7}$$

which, when combined with Eq. (A1), give

$$(s_A|e^{-\alpha_3 r_C^2}|s_B) = \exp[-\alpha_1\overline{AE}^2 - \alpha_2\overline{BE}^2 - \alpha_3\overline{CE}^2]\int e^{-\alpha_T r_E^2} d\tau$$
$$= (\pi/\alpha_T)^{3/2}\exp[-\alpha_1\overline{AE}^2 - \alpha_2\overline{BE}^2 - \alpha_3\overline{CE}^2]. \quad \text{(A8)}$$

To evaluate (A2) we introduce

$$\vec{D} = (\alpha_1\vec{A} + \alpha_2\vec{B})/(\alpha_1 + \alpha_2), \quad \text{(A9)}$$

and take the z axis along $\overrightarrow{CD}$ so that

$$\left(s_A\left|\frac{1}{r_C}e^{-\alpha_3 r_C^2}\right|s_B\right) = \exp(-\alpha_1\overline{CA}^2 - \alpha_2\overline{CB}^2)\int e^{-\alpha_T r_C^2} r_C^{-1} e^{2(\alpha_1+\alpha_2)\vec{r}_C\cdot\vec{CD}} d\tau$$
$$= 2\pi\exp(-\alpha_1\overline{CA}^2 - \alpha_2\overline{CB}^2)\int_0^\infty\int_{-1}^1 e^{-\alpha_T r_C^2} r_C e^{2(\alpha_1+\alpha_2)\overline{CD}r_C\cos\theta} d(\cos\theta)\, dr_C$$
$$= \left(\frac{\pi}{(\alpha_1+\alpha_2)\overline{CD}}\right)\exp(-\alpha_1\overline{CA}^2 - \alpha_2\overline{CB}^2)\int_0^\infty e^{-\alpha_T r^2}(e^{2(\alpha_1+\alpha_2)\overline{CD}r} - e^{-2(\alpha_1+\alpha_2)\overline{CD}r})\, dr. \quad \text{(A10)}$$

Upon letting

$$\beta = (\alpha_1+\alpha_2)\overline{CD}/\alpha_T, \quad \text{(A11)}$$

$$t = \sqrt{2}\,(\alpha_1+\alpha_2)\overline{CD}/\sqrt{\alpha_T}, \quad \text{(A12)}$$

the above integral reduces to

$$\left(s_A\left|\frac{1}{r_C}e^{-\alpha_3 r_C^2}\right|s_B\right) = \left(\frac{\pi}{(\alpha_1+\alpha_2)\overline{CD}}\right)\exp\left(-\alpha_1\overline{CA}^2 - \alpha_2\overline{CB}^2 + \frac{(\alpha_1+\alpha_2)^2\overline{CD}^2}{\alpha_T}\right)\left(\int_{-\beta}^\infty e^{-\alpha_T y^2} dy - \int_\beta^\infty e^{-\alpha_T y^2} dy\right)$$
$$= \left(\frac{2\pi}{\alpha_T t}\right)\exp\left(-\alpha_1\overline{CA}^2 - \alpha_2\overline{CB}^2 + \frac{(\alpha_1+\alpha_2)^2\overline{CD}^2}{\alpha_T}\right)\int_0^t e^{-z^2/2} dz. \quad \text{(A13)}$$

The matrix elements involving p-type Bloch sums can be deduced from Eqs. (A8) and (A13) by an appropriate differentiation since a p-type GTO is related to an s-type Gaussian as

$$x_A e^{-\alpha_1 r_A^2} = \frac{1}{2\alpha_1}\frac{\partial}{\partial A_x}e^{-\alpha_1 r_A^2},$$

where x_A and A_x are the x component of $\vec{r}_A$ and $\vec{A}$. The procedures for calculating overlap and kinetic-energy matrix elements are much simpler and have been given in Ref. 17.

---

*Work supported by the Wisconsin Alumni Research Foundation through the University of Wisconsin Research Committee and by the NSF.

[1]*Electronic and Structural Properties of Amorphous Semiconductors*, edited by P. G. LeComber and J. Mort (Academic, New York, 1973).

[2]*Proceedings of the Fifth International Conference on Amorphous and Liquid Semiconductors, Garmisch-Partenkirchen, West Germany, 1974*, edited by J. Stuke and W. Brenig (Taylor and Francis, London, 1974).

[3]AIP Conf. Proc. 20, (1974).

[4]See, for example, S. C. Moss and J. F. Graczyk, in *Proceedings of the Tenth International Conference on the Physics of Semiconductors, Cambridge, Mass., 1970*, edited by S. P. Keller, J. C. Hensel, and F. Stern (U. S. AEC, Oak Ridge, Tenn., 1970), p. 658; N. J. Shevchik and W. Paul, J. Non-Cryst. Solids 8-10, 381 (1972).

[5]D. E. Polk, J. Non-Cryst. Solids 5, 365 (1971); D. E. Polk and D. S. Boudreaux, Phys. Rev. Lett. 31, 92 (1973).

[6]D. Henderson and F. Herman, J. Non-Cryst. Solids 8-10, 359 (1972).

[7]D. Henderson, J. Non-Cryst. Solids 16, 317 (1974).

[8]P. Steinhardt, R. Alben, and D. Weaire, J. Non-Cryst. Solids 15, 199 (1974).

[9]G. A. N. Connell and R. J. Temkin, Phys. Rev. B 9, 5323 (1974).

[10]D. L. Evans, M. P. Teter, and N. F. Borrelli, J. Non-Cryst. Solids 17, 245 (1975).

[11]D. Beeman and B. L. Bobbs, Phys. Rev. B 12, 1399 (1975).

[12]See, for example, M. E. Thorpe and D. Weaire, in Ref. 2, p. 917, and the references given therein.

[13]I. B. Ortenburger and D. Henderson, Phys. Rev. Lett.

30, 1047 (1973); D. Henderson and I. B. Ortenburger, in *Computational Method for Large Molecules and Localized States in Solids*, edited by F. Herman, A. D. McLean, and R. K. Nesbet (Plenum, New York, 1973); J. Phys. C 6, 631 (1973).
[14]R. Alben, S. Goldstein, M. F. Thorpe, and D. Weaire, Phys. Status Solidi B 53, 545 (1972).
[15]J. D. Joannopoulos and M. L. Cohen, Phys. Rev. B 7, 2644 (1973).
[16]E. E. Lafon and C. C. Lin, Phys. Rev. 152, 579 (1966).
[17]R. C. Chaney, T. K. Tung, C. C. Lin, and E. E. Lafon, J. Chem. Phys. 52, 361 (1970).
[18]W. Y. Ching and J. Callaway, Phys. Rev. Lett. 30, 441 (1973).
[19]W. Y. Ching and J. Callaway, Phys. Rev. B 11, 1324 (1975); 9, 5115 (1974).
[20]R. C. Chaney, C. C. Lin, and E. E. Lafon, Phys. Rev. B 3, 459 (1971).
[21]J. Callaway and C. S. Wang, Phys. Rev. B 7, 1096 (1973).
[22]R. A. Tawil and J. Callaway, Phys. Rev. B 7, 4242 (1973).
[23]J. Rath and J. Callaway, Phys. Rev. B 8, 5398 (1974).
[24]R. A. Tawil and S. P. Singhal, Phys. Rev. B 11, 699 (1975).
[25]R. C. Chaney, E. E. Lafon, and C. C. Lin, Phys. Rev. B 4, 2734 (1971).
[26]U. Seth and R. Chaney, Phys. Rev. B 12, 5923 (1975).
[27]J. E. Falk and R. J. Fleming, J. Phys. C 6, 2954 (1973).
[28]W. Y. Ching and C. C. Lin, Phys. Rev. Lett. 34, 1223 (1975).
[29]W. Y. Ching and C. C. Lin, Phys. Rev. B 12, 5536 (1975).
[30]W. P. Menzel, K. Mednick, C. C. Lin, and C. F. Dorman, J. Chem. Phys. 63, 4708 (1975).
[31]J. E. Simmons, C. C. Lin, D. F. Fouquet, E. E. Lafon, and R. C. Chaney, J. Phys. C 8, 1549 (1975).
[32]D. J. Stukel and R. N. Euwema, Phys. Rev. B 1, 1635 (1970).
[33]See, for example, J. Callaway, *Quantum Theory of the Solid State* (Academic, New York, 1974), p. 188.
[34]L. Ley, S. Kowalczyk, R. Pallak, D. A. Shirley, Phys. Rev. Lett. 29, 1008 (1972).
[35]F. C. Brown and O. P. Rustgi, Phys. Rev. Lett. 28, 497 (1972).
[36]D. Engemann and R. Fisher, in Ref. 2, p. 947.
[37]W. E. Spear and P. G. LeComber, J. Non-Cryst. Solids 8-10, 727 (1972).
[38]W. E. Spear, in Ref. 2, p. 1.
[39]J. E. Fischer and T. M. Donovan, J. Non-Cryst. Solids 8-10, 202 (1972).
[40]D. J. Pierce and W. E. Spicer, Phys. Rev. B 5, 3017 (1972).
[41]B. Y. Tong, in Ref. 3, p. 145.
[42]R. P. Messmer and G. D. Watkins, Phys. Rev. B 7, 2568 (1973).
[43]M. F. Thorpe, D. Weaire, and R. Alben, Phys. Rev. B 7, 3777 (1973).